Modulation of Quantum Yield of Primary Radical Pair Formation in Photosystem II by Site-Directed Mutagenesis Affecting Radical Cations and Anions†

Stephen A. P. Merry, Peter J. Nixon, Laura M. C. Barter, Maria Schilstra, George Porter, James Barber, James R. Durrant, and David R. Klug*

Molecular Dynamics and Photosynthesis Research Groups, Centre for Photomolecular Sciences, Departments of Biochemistry and Chemistry, Imperial College, London, SW7 2AY, U.K.

Received March 3, 1998; Revised Manuscript Received October 6, 1998

ABSTRACT: Pigment−protein interactions play a significant role in determining the properties of photosynthetic complexes. Site-directed mutants of *Synechocystis* PCC 6803 have been prepared which modify the redox potential of the primary radical pair anion and cation. In one set of mutants, the environment of P680, the primary electron donor of Photosystem II, has been modified by altering the residue at D1-His198. It has been proposed that this residue is an axial ligand to the magnesium cation. In the other set, the D1-Gln130 residue, which is thought to interact with the C9-keto group of the pheophytin electron acceptor, has been changed. The effect of these mutations is to alter the free energy of the primary radical pair state, which causes a change in the equilibrium between excited singlet states and radical pair states. We show that the free energy of the primary radical pair can be increased or decreased by modifications at either the D1-His198 or the D1-Gln130 sites. This is demonstrated by using three independent measures of quantum yield and equilibrium constant, which exhibit a quantitative correlation. These data also indicate the presence of a fast nonradiative decay pathway that competes with primary charge separation. These results emphasize the sensitivity of the primary processes of PS II to small changes in the free energy of the primary radical pair.

The ability of higher plants, cyanobacteria, and algae to oxidize water during photosynthesis has led to their global proliferation. The splitting of water occurs in the multiprotein complex known as photosystem II (PS II[1]). Following the transfer of excitation energy to the reaction center of PS II, an ultrafast charge separation forms a primary radical pair state. This charge-separated state is then further stabilized by the subsequent secondary electron-transfer reactions (*1*).

It is possible to isolate a PS II reaction center complex from thylakoid membranes consisting of just the D1, D2, and cytochrome b-559 polypeptides (*2*, *3*). This is the minimal charge-transferring complex of PS II, and is generally accepted to bind 6 chlorophyll a, 2 pheophytin a, 2 β-carotene and 1 cytochrome b-559 (*4*, *5*). During the isolation procedure, both of the quinone electron acceptors and the manganese-based oxygen-evolving complex (OEC) are lost. The redox-active tyrosine is still present in this complex, but it is nonfunctional. The primary radical pair state is formed when P680, the primary electron donor in PS II, transfers an electron to the pheophytin primary electron acceptor with a dominant time constant of 21 ps (*6*, *7*). The absence of the secondary electron acceptor means that the primary radical pair has a lifetime of tens of nanoseconds. This state recombines to ground with time constants of approximately 20 and 50 ns (*8*, *9*).

Site-directed mutagenesis can be employed to change the pigment−protein interactions in photosynthetic complexes (*10*−*12*). Cyanobacteria are convenient organisms to study, in particular *Synechocystis* PCC 6803 and *Synechococcus* PCC 7002, because they are readily transformed (*13*). Both of these cyanobacteria have a natural DNA uptake system that allows transformation by addition of exogenous DNA. The cyanobacterium *Synechocystis* PCC 6803 has previously been used to study secondary electron-transfer reactions in PSII (*11*) and to probe the function of the OEC (*12*). More recently, we have looked at the effect of site-directed mutagenesis upon the primary charge separation in isolated PS II reaction centers (*14*).

To date, the structure of the PS II reaction center has not been solved to atomic resolution. However the structures of reaction centers from the purple bacteria *Rhodopseudomonas* (*Rps.*) *viridis* (*15*) and *Rhodobacter* (*Rb.*) *sphaeroides* (*16*) and PS I (*17*) are available. It has been noted that there is significant localized similarity in the primary structure between the D1 and D2 polypeptides of the PS II reaction center and the L and M subunits in purple bacteria (*18*). The electron acceptor side of the reaction centers of PS II and purple bacteria show similarities in the cofactors and their function (*19*).

A comparison of the sequence of the D1 and D2 polypeptides of *Synechocystis* PCC 6803 with those of higher plants reveals several significant differences. The residues at D1-Gln130 and D1-His198 are of particular significance to this

† This study was financially supported by the BBSRC, BOC, RITE, EU, and the Royal Society. J.R.D. is a BBSRC Advanced Research Fellow.

* Corresponding author: Centre for Photomolecular Sciences, Departments of Biochemistry and Chemistry, Imperial College, London, SW7 2AY, U.K. Fax: 44171-594-5806. E-mail: d.klug@ic.ac.uk.

[1] Abbreviations: PS II, photosystem two; OEC, oxygen-evolving complex.

10.1021/bi980502d CCC: $15.00
Published on Web 11/20/1998

paper. In *Synechocystis* the residue at D1-Gln130 is a glutamine, but in *Pisum sativum* (pea, a higher plant), it is a glutamate residue. This amino acid is likely to form a hydrogen bond to the C9-keto group of the pheophytin primary electron acceptor (*20*) as is the case in the analogous residue L-104 in the purple bacterium *Rb. capsulatus*. The mutation of L-104 in *Rb. capsulatus* from a glutamate to a glutamine or leucine residue causes the pheophytin Q_x absorbance band to shift to the blue, but the charge separation rate was reported to remain unaffected (*21*). When the D1-Gln130 residue in the wild-type *Synechocystis* was changed to glutamate we observed a red shift in the pheophytin Q_x transition. When the residue was changed to leucine, a blue shift was observed (*14*). These observations strongly suggest that this residue binds to the pheophytin via a hydrogen bond.

In the reaction centers from *Rb. sphaeroides* and *Rps. viridis*, the histidine residue at L-173 forms an axial ligand to the magnesium atom in one of the chlorophylls which composes the primary donor. Drawing upon the analogy between the purple bacteria and PS II, the D1-His198 residue is proposed to ligate to the corresponding chlorophyll molecule in PS II. It has been shown that, in the D1-His198Ala mutant, the chlorophyll to pheophytin stoichiometry is unperturbed (Nixon and Diner, unpublished data). It is therefore likely that, as in the case of the L-His173Gly in *Rb. sphaeroides* reaction centers (*22*), a water molecule is the adventitious ligand that replaces histidine in this mutant and binds to the magnesium atom. This cavity mutant L-His173Gly seemed to have little effect on the optical and redox properties of the primary donor.

We have previously reported a study of the effect of mutations at the D1-130 residue upon the primary photochemistry of the PSII reaction center (*14*). In this paper we extended this work by the study of the D1-198 mutants. We find remarkably similar effects on the primary photochemistry for mutations at either site, and conclude that the primary effect of these mutations is to moderate the free energy of the $P_{680}{}^{+}Ph^{-}$ radical pair state.

MATERIALS AND METHODS

Two strains of *Synechocystis* PCC 6803 have been used to obtain reaction centers, TC31 and TC35 (*23*). These are deletion mutants containing only one copy of the three *psbA* genes responsible for D1 synthesis (*psbA3*). The genotype of both strains is identical. These two independent transformants were analyzed to investigate the degree of variation in the preparation of the samples and also to give a measure of the spread of the data. Mutants at D1-Gln130 and D1-His198 residue were generated as described in ref *23* and the PS II reaction centers isolated, as described in ref *14*. Preliminary characterization of the D1-His198 mutants is described in ref *24*. The wild-type *Synechocystis* reaction center contains 7−8 chlorophyll a, 2 pheophytins, 1 β-carotene, and 1 cytochrome b-559. This composition is similar to that for the higher plant reaction center (*4*) except for 1−2 extra chlorophylls and reduced carotenoid content. The preparation also contains some additional contaminating polypeptides. The pigment stoichiometry for all of the mutant reaction centers was similar to that for the *Synechocystis* wild type.

In all of the experiments the samples were resuspended in a buffer containing 50 mM Mes-NaOH, 20 mM sodium pyrophosphate, 1 mM ϵ-amino caproic acid, and 1 mM benzamidine at pH 6.5 (*14*). Anaerobic conditions were achieved by the addition of 5 mM glucose, 0.1 mg mL^{-1} glucose oxidase, and 0.05 mg mL^{-1} catalase. The position of the chlorophyll Q_y band absorption maximum was used as a monitor of the stability of the sample; this peak shifted by less than 1 nm during the course of the experiments, suggesting an activity loss of less than 10% (*8*).

Nanosecond measurements were performed as described in ref *14*. Briefly, the 500 ps pulse at 2 Hz, from a dye laser pumped by Nitrogen laser, was used to excite the samples. The samples were excited using 680 nm excitation (44 $\mu J/cm^2$) which provided nonsaturating pulses. The probe wavelength was 820 nm, and the path length of the cell was 4 mm. All samples contained 2 μg of chlorophyll and had the same optical density at the excitation wavelength. The average of 100 flashes was analyzed to a sum of three exponential components. In these fits, one lifetime was fixed to 4.7 μs to represent the electronically filtered decay of the $P680^3$ state. All other parameters were free-running.

The single-photon counting apparatus has been fully described in ref *25*. A Modelocked Coherent YAG laser synchronously pumps a DCM dye laser. The cavity dumped output has a repetition rate of 5 MHz and an 8 ps pulse duration. The instrument response was measured to be 36 ps using a LUDOX scattering solution. The biological samples were excited at 684 nm, and the fluorescence was monitored after a 720 nm high pass filter. The incident light intensity was 3.44×10^{15} photons/s in a volume of 0.2 cm^3, and the sample OD was equal to 0.1 at the excitation wavelength.

For the picosecond transient absorption spectroscopy, the samples were resuspended to give a final chlorophyll concentration of 30 μg mL^{-1}. Samples were mounted in a cylindrical cuvette (path length 2.5 mm) which was rotated at a sufficient speed to exchange the excited sample volume between excitation pulses. The excitation pulses were chosen for selective excitation of P680; for a more detailed discussion refer to ref *26*. Samples were maintained at ~10 EC during each experiment and had an optical absorption of between 0.5 and 1.0 at 676 nm.

Transient absorption data were collected as described previously (*7*). The instrument response was 120−250 fs depending upon probe wavelength. Zero time delay was determined using dye standards. Data were collected on a 0−60 ps time scale at 150 time delays. All data was collected with the magic angle between pump and probe beams to avoid contributions from any depolarization processes. The data were globally analyzed assuming multiexponential kinetics (*7*).

Analysis of Picosecond Transient Absorption Data and Calculation of Thermodynamic Parameters: Optical Excitation Results in the Formation of the Singlet Excited State of the Reaction Center, RC.* Primary charge separation proceeds from this manifold of RC* states to generate the primary radical pair state, RP.

$$RC^* \leftrightarrow RP$$

This equilibrium is characterized by the equilibrium constant,

K, where

$$K = \frac{[\mathrm{RP}]}{[\mathrm{RC}^*]}$$

The equilibrium constant is related to the free-energy change of radical pair formation ΔG.

$$\Delta G = -k_B T \ln K$$

The dominant time constant associated with the formation of the primary radical pair state in PSII reaction centers isolated from peas is 21 ps (*6*, *7*) with a small 3 ps component also present. The data at early times ($\ll$3 ps) will therefore consist solely of a singlet state spectrum of the RC and minimal RP formation. The data at 60 ps after excitation will show the spectral changes associated with the equilibrium between RC* and RP.

The state spectrum for the excited singlet states and radical pair spectrum for the Q_x region can be extracted from the data on the *P. sativum* reaction center. This use of the extracted spectra from *P. sativum* is clearly an approximation and may account to some extent for the limited quality of the simulation obtained. However it is also clear from the results that the simulation is a reasonable fit, and it would therefore seem that this approximation is valid. The singlet state spectrum used in this simulation (ΔOD_{RC*}) is the ΔOD at 1 ps following excitation. There is extensive energy equilibration prior to charge separation, but by this time, the vast majority of equilibration is completed (*27*, *28*). The ΔOD_{RP} spectrum corresponds to the absorbance changes expected for unity radical pair formation (calculated from the 60 ps ΔOD spectrum obtained for *P. sativum* using an equilibrium constant of $K = 3$ at this time (*29*). The transient spectrum at any given time consists of a linear combination of ΔOD_{RC*} and ΔOD_{RP} spectra. For all reaction centers, the spectrum at 60 ps can then be fit using the following relationship:

$$\Delta OD_{60\ ps} = \beta^*(\Delta OD_{RP}) + (1 - \beta)(\Delta OD_{RC*})$$

where β is the percentage of the equilibrated ensemble found in the radical pair state at this time. The fitting procedure was performed to optimize the quality of fit over as much of the region of the pheophytin anion bleach and surrounding area as possible. In addition it is possible to simulate the 18−30 ps kinetic spectra of all of the preparations. The kinetic spectra are fit using the following equation:

$$\Delta OD_{ks} = (\text{singlet loss})(\Delta OD_{RC*}) - \beta \Delta OD_{RP}$$

where singlet loss is the complete loss of singlet states from the system and ΔOD_{ks} is the amplitude of the simulated spectrum.

In the stimulated emission sideband, the total singlet state loss from the system is monitored. By applying the same principles employed for the fit to the nondecaying component in the Q_x region, one can simulate these spectra. From this fit to the data, the equilibrium constant 60 ps after excitation can be quantified.

RESULTS

Two sets of site-directed mutants from *Synechocystis* PCC 6803 were studied. In one set the pigment−protein interactions of the primary donor of PS II have been modified by altering the amino acid at D1-His198. This residue at D1-His198 is thought to form an axial bond to the central metal ion of a chlorophyll macrocycle. In the other set of mutants, the interactions of the pheophytin primary electron acceptor are modified via the D1-Gln130 residue.

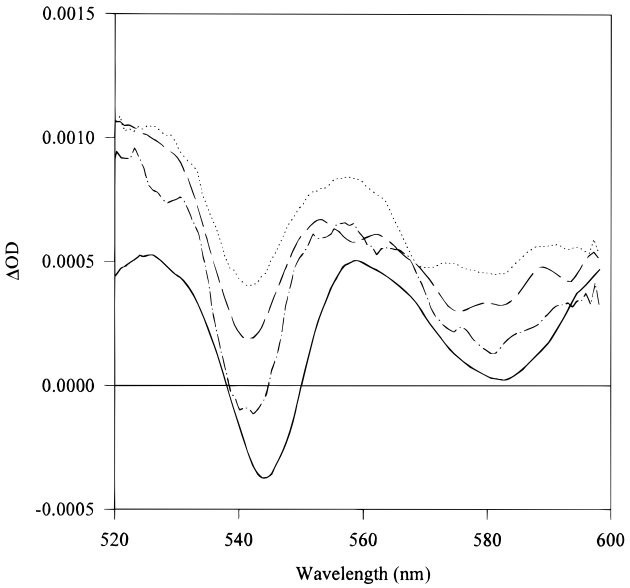

FIGURE 1: The transient spectra at 60 ps for the isolated PSII reaction centers from *P. sativum* (—), *Synechocystis* TC35 wild type (− − −), the D1-His198Ala mutant (− · −), and the D1-His198Gln mutant (···).

Picosecond Transient Absorption Measurements. We have previously reported picosecond and nanosecond transient absorption data from PS II reaction centers isolated from TC31 wild type and D1-Gln130 mutant strains of *Synechocystis* (*14*). The corresponding data for the D1-His198Ala and D1-His198Gln mutants are shown in Figures 1 and 2. The previously published data from the *P. sativum* reaction center is also shown for comparison (*14*). Figure 1 presents the picosecond transient absorption data collected between 520 and 600 nm, the region of the chlorin Q_x absorption bands. Kinetic analysis of data collected on a 0−60 ps time scale determined that, the kinetics of both the wild type and D1-His198 mutant *Synechocystis* reaction centers are adequately fit by a monoexponential component with a lifetime of between 18 and 30 ps, as we have reported previously for the D1-130 mutants. The transient spectra following the decay of this component (time delay of 60 ps) are shown in Figure 1. It is not clear whether the spread of lifetimes of the 18−30 ps component is genuine or (more likely) reflects an imprecision due to the limited signal-to-noise ratio of the data. Moreover, the *P. sativum* reaction centers show the presence of an additional small component of 1−3 ps (*7*). The poorer signal-to-noise ratio of the *Synechocystis* data presented here (due to limited quantities of sample) precludes the detection of a small 1−3 ps component.

In addition to shifts in the position of the Q_x absorption bleach between these samples, it is possible to simulate the differences in amplitude of this bleach relative to the positive absorption changes attributed to excited/cation/anion states. This can be achieved by simulating these spectra as superpositions of spectra due to singlet excited states and

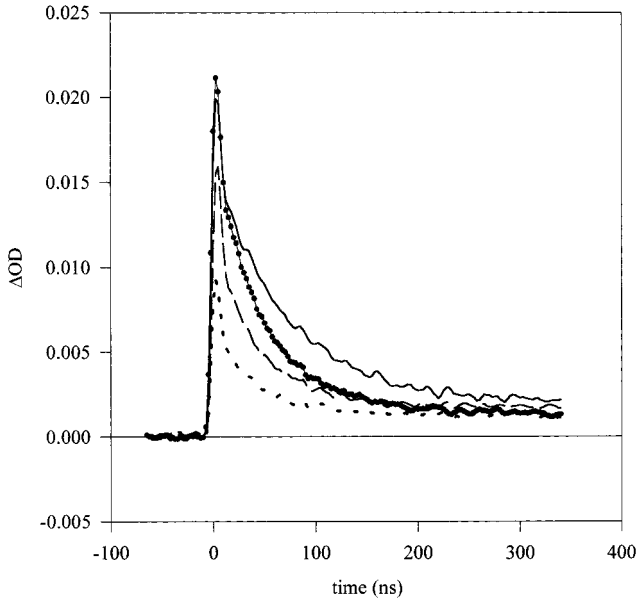

FIGURE 2: Nanosecond quantum yield measurements carried out on the higher plant reaction center (—●—), *Synechocystis* TC35 type (– – –), the D1-His198Ala mutant (—), and the D1-His198Gln mutant (•••). The samples were excited using nonsaturating flashes. The data have been scaled to the same number of photons absorbed, and hence the amplitude of the signals is proportional to the quantum yield of primary charge separation on this time scale.

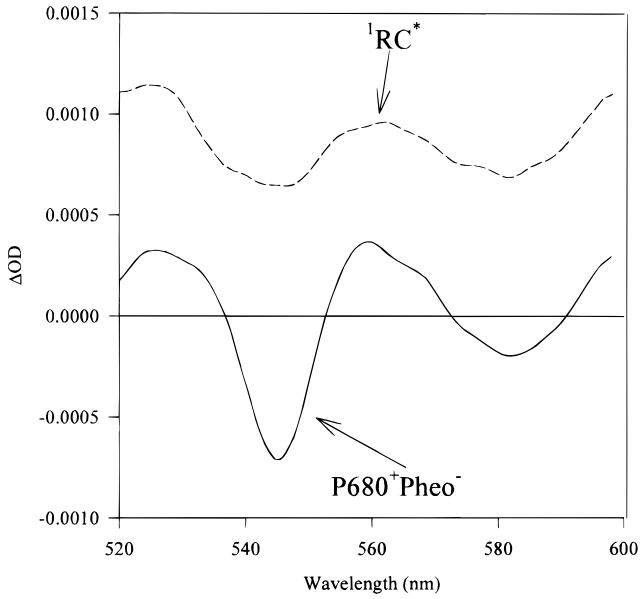

FIGURE 3: The state spectra used in a linear combination to simulate the transient spectra and the kinetic spectra for in the Q_x region. The RC* spectrum (– – –) is the transient spectrum at 1 ps, and the radical pair spectrum (—) shows the absorbance changes associated with 100% primary radical pair formation. The origin of the two spectra is discussed in the text.

radical pair states, as detailed in the materials and methods. These spectra are shown in Figure 3. It is thus possible to calculate the equilibrium constant between the singlet excited states and the primary radical pair from these transient absorption spectra at 60 ps. A typical fit to the transient data from the D1-His198Ala mutant is shown in Figure 4. The resulting percent proportions of radical pairs formed at 60 ps for each of the reaction center samples are shown Table 1 (column 2). On the whole, this analysis is able to

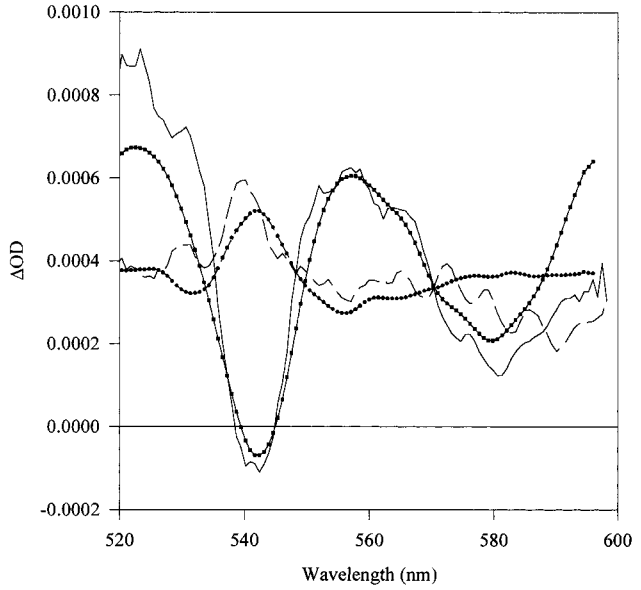

FIGURE 4: Results of a typical simulation of the transient data from the D1-His198Ala mutant. The experimental nondecaying component at 60 ps (—) and the spectra of the 18 ps kinetic component (– – –) are shown along with the simulated nondecaying component (—■—) and kinetic spectra (—●—).

reproduce the essential features of the spectra, and in particular the relative amplitudes of the pheophytin Q_x and chlorophyll Q_x bleaches, and the amplitude of the positive background.

The calculated ΔG values from this fit to the 60 ps data are presented in Table 1, column 4. The error of the simulation of percentage singlet states is estimated to be ±10%. It should be borne in mind that the free energy of the radical pair state is likely to be time-dependent, with dynamic relaxation of the protein matrix being associated with time constants of tens and hundreds of picoseconds. The free energies obtained by the simulation are only valid at 60 ps. Analysis of nanosecond single-photon counting measurements has indicated a ΔG of ~100 mV for *P. Sativum*, indicating a significant relaxation of the radical pair free energy by this time scale (*25*).

The presence of singlet excited states can be monitored by the stimulated emission sideband at 730 nm (*30*). In common with the Q_x region, the data for all of the preparations can be fitted to a monoexponential lifetime of between 18 and 30 ps and a nondecaying component (data not shown). The amplitude of the signal in the stimulated emission sideband is determined by the equilibrium constant between the singlet excited states and the radical pair: the larger the amplitude of the emission sideband, at 730 nm, the greater the equilibrium constant. The amplitude of the transient spectra at 60 ps differs in the mutants. The amplitude of this feature is correlated with the nanosecond quantum yield of primary radical pairs previously reported in ref *14*. This correlation is also evident in Table 1.

Significant shifts are obtained in the pheophytin Q_x absorption band upon the mutation of the D1-Gln130 residue. The peak of the bleach in the Q_y region is changed by <1 nm from the higher plant reaction center upon mutation of either the D1-Gln130 or the D1-His198 residue. Given the high degree of spectral overlap at this wavelength and the extensive mixing of site energies caused by dipole−

Table 1: Summary of the Results Obtained by Picosecond and Nanosecond Transient Absorption Studies and Time-Correlated Single-Photon Counting[a]

preparation	radical pair states[b] (%)		ΔG at 60 ps[c] (meV)	nanosecond quantum yield of radical pairs[d] (%)	singlet states at 80 ± 30 ps[e] (%)	nonradiative singlet state decay (%)	
	Q_x region	Q_y region				at 60 ps[f]	from 18 to 30 ps component[g]
D1-Gln130Leu	5	26	+74	46	59	36	45
D1-His198Gln	18	34	+37	46	48	34	13
wild-type TC31	28	45	+24	60	*h*	*h*	27
wild-type TC35	32	38	+18	75	47	21	4
D1-His198Ala	54	68	−5	94	45	1	9
D1-Gln130Glu	65	60	−15	65	35	0	0
Pisum sativum	75	75	−27	100	25	0	0

[a] For all calculations the equilibrium constant in the isolated reaction center from *Pisum sativum* at 60 ps was assumed to equal 3 (as established previously). [b] Calculated from the fit to the 60 ps transient spectra. [c] Calculated from the fit to the 60 ps transient spectra in the Q_x spectral region (col 2). [d] Measured from the total amplitude of the nanosecond transient absorption decay. [e] Measured by time-resolved fluorescence. [f] Calculated by the following: 1 − (col 2) − (col 6). [g] Calculated from the 18−30 ps kinetic spectra in the Q_x region. [h] Data not available.

dipole coupling (*31*), this result is not altogether unexpected.

Nanosecond Transient Absorption Measurements. The primary radical pair state absorbs at 820 nm. By using nanosecond transient absorption measurements with nonsaturating flashes, it is possible to obtain the relative quantum yield of radical pair formation at this wavelength (*14*). The data collected from the D1-His198 mutants is shown in figure 2 and is compared with wild-type TC35 *Synechocystis* and the higher plant *P. sativum* reaction centers.

The nanosecond transient absorption data were fitted to three exponential components. In these fits, one lifetime was fixed at 4.7 μs, to represent the electronically filtered decay of the P680 triplet state, while all other parameters were free-running. The two free-running lifetimes were found to be in the ranges of 4.5−6.5 and 35−50 ns. The nanosecond components monitor the charge recombination of the primary radical pair state. Either the initial absorbance change or the amplitudes of the nanosecond components can be used as a measure of the quantum yield of radical pair formation. The total amplitudes of the decays are presented in Table 1. These values have been normalized to 100% for the ϕ_{RP} in the isolated *P. sativum* reaction centers (*8*).

The nanosecond measurements indicate that it is possible to enhance the yield of primary radical pair formation in isolated reaction centers above that of the wild-type organism by site-directed mutagenesis. The nanosecond quantum yield can be modified by changing the residue binding to either the primary electron donor or the primary electron acceptor. On modifying a proposed axial ligand to P680 at D1-His198, the relative nanosecond quantum yield is *Pisum sativum* > *Synechocystis* D1-His198Ala > wild-type *Synechocystis* > D1-His198Gln mutant (see Table 1). When the residue attached to the Pheophytin electron acceptor is changed from glutamine to the glutamate residue, as found in the higher plant reaction center, the efficiency of primary charge separation is also enhanced. It has been demonstrated that the yield of primary charge separation upon mutation of the D1−130 residue is *P. sativum* > D1-Gln130Glu > wild-type *Synechocystis* > *Synechocystis* D1-Gln130Leu (*14*).

The trends in the nanosecond quantum yield are reproduced in the picosecond data. The size of the pheophytin anion bleach in the Q_x region is proportional to the nanosecond quantum yield of the D1−198 mutants (see Figure 1. Also compare columns 2 and 5 of Table 1.). The equilibrium constant at 60 ps derived from the stimulated emission sideband also correlates with the nanosecond quantum yield for the D1-Gln130 and the D1-His198 mutants (see Table 1).

The nanosecond transient absorption data indicates that both strains of the *Synechocystis* wild-type reaction center show a nanosecond quantum yield, which is 0.60% that of the higher plant reaction center. A similar level of activity was observed in the *Synechocystis* reaction centers isolated by others on the basis of pheophytin anion photoaccumulation experiments (*32*). This yield is surprisingly low considering that the quantum yield is approximately 1.0 in the higher plant reaction center and the reaction center from *Chlamydomonas reinhardtii.*

Time-Correlated Single-Photon Counting. The time-resolved fluorescence data collected from all preparations is presented in Figure 5. This technique has been used to make a quantitative comparison of the singlet state population with the use of dye standards. The fluorescence yield (area under the curves) varies considerably between the different preparations. The relative fluorescence amplitudes of these samples are tabulated in Table 1, column 6, for a time delay of 80 ps. They have been calculated using the data from *P. sativum* as a standard (*8*). This time delay corresponds closely with the 60 ps time delay employed in the analysis of the picosecond transient absorption data. In particles with a high quantum yield of radical pair formation, the fluorescence yield should be smaller than in those with a low yield of radical pairs. We find that this is indeed the case. The higher plant reaction center, with the largest quantum yield of radical pair formation, is the least fluorescent. The D1-Gln130Leu mutant, with the lowest quantum yield, has the highest fluorescence. The wild-type *Synechocystis* preparation is approximately twice as fluorescent as the higher plant reaction center.

DISCUSSION

Picosecond and nanosecond transient absorption spectroscopy combined with time-correlated single-photon counting have been employed to study two sets of site-directed mutants from *Synechocystis* PCC 6803. In one set of mutants, the environment of P680, the primary electron donor of photosystem II, has been modified by altering the residue at D1-His198. In another set of mutants, D1-Gln130 residue, which binds the pheophytin primary electron acceptor, has been transformed.

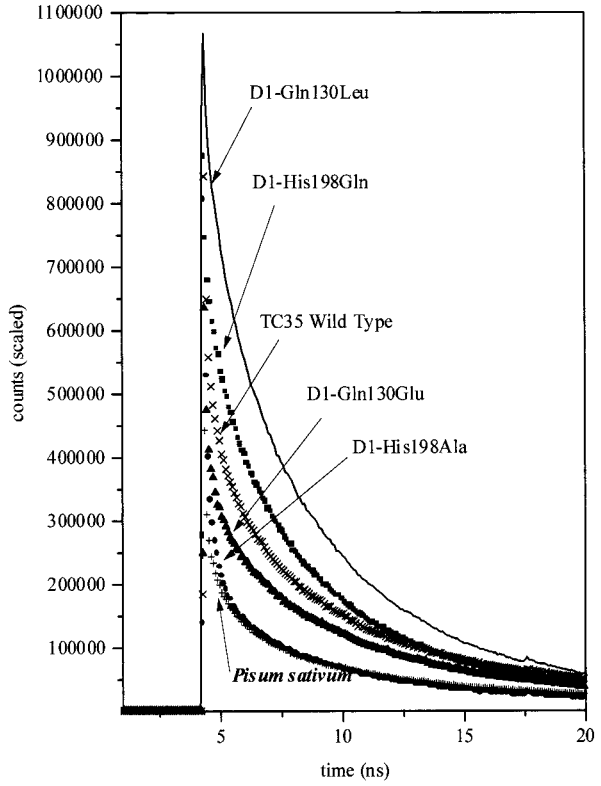

FIGURE 5: Time-resolved fluorescence decays of mutants and wild-type *Synechocystis* reaction centers collected using the technique of single-photon counting. The data have been scaled to the same number of photons absorbed and therefore indicate the relative population of chlorin singlet states following excitation: (—) D1-Gln130Leu mutant, (■) D1-His198Gln mutant, (×) wild-type TC35 *Synechocystis*, (▲) D1-Gln130Glu mutant, (●) D1-His198Ala mutant, and (+) *Pisum sativum.*

The results of our analysis are summarized in Table 1. A correlation diagram showing all of the data is shown in Figure 6. The data (shown in terms of radical pair population) is plotted against the radical pair population calculated from the fit to the 60 ps spectral component in the Q_y region. A linear fit to the data is shown, and on comparison to the function $y = x$, it is clear that four independent measurement methods and analysis techniques (time-resolved fluorescence, nanosecond transient absorption, and picosecond transient absorption in two spectral regions) all agree quantitatively regarding the relative concentrations of radical pair and singlet states. There is a slight discrepancy between the results from the analysis of the 60ps component in the Q_x and the Q_y regions, (Table 1, columns 2 and 3). A possible cause of this discrepancy could be due to the effect of varying contributions of P^+Chl^- states. Studies involving simulations of these data are in progress and will be reported in a future paper. Our analysis of the picosecond data is based upon the variations in the equilibrium constant between singlet states and radical pair states at 60 ps. This variation in equilibrium constant can be most easily rationalized in terms of variations in the free energy of the primary radical pair state at this time.

We have previously considered in detail the singlet state/radical pair equilibria formed in PS II reaction centers isolated from higher plants (*29*, *33*). We have previously found, on the basis of fluorescence up conversion data, the equilibrium constant between singlet and radical pair states at 60 ps to be 3:1, which is the same as the equilibrium

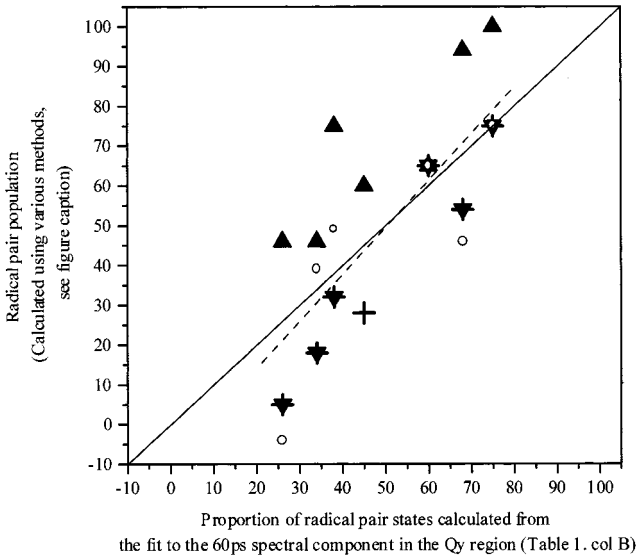

FIGURE 6: Correlation diagram showing the following data plotted against the proportion of radical pair states calculated from the fit to the 60 ps spectral component in the Q_y region (Table 1, column 3). It should be noted that the values in column 2 were used to calculate some of the results shown in Table 1. Therefore column 3 has been used as the reference in this figure. (i) Proportion of radical pair states calculated from the fit to the 60 ps spectral component in the Q_x region (Table 1, column 2), (+), and (ii) proportion of radical pairs calculated from the time-resolved fluorescence data (Table 1, column 6), combined with the proportion of nonradiative singlet-state decay associated with the 18−30 ps kinetic spectra (Table 1, column 8), (○). (iii) Nanosecond quantum yield of radical pair states (Table 1, column 5) (▲). The linear fit to the above data is shown (− − −), along with the function $y = x$ (—).

constant reported here from simulation of the transient absorption data. This equilibrium constant corresponds to a free-energy gap between singlet and radical pair states of 27 meV at this time. On longer, nanosecond, time scales this ΔG increases to ~100 meV (*25*). This increase in ΔG with time can most probably be attributed to a dynamic relaxation of the radical pair free energy (*33*, *34*), although some influence from static disorder on the transient data cannot be ruled out. The variation in equilibrium constant between the different reaction center preparations studied here can be attributed to the variation in radical pair free energy, resulting from shifts in the redox potentials of $P680^+$ and Ph^-.

Picosecond and nanosecond transient absorption studies combined with time-correlated single-photon counting have all implied the same trends in the activity of the isolated PS II reaction centers from mutant and wild-type *Synechocystis*. The yield of primary radical pair formation in the wild-type organism (either TC31 or TC35) is approximately half of that observed in higher plant reaction centers.

The primary radical pair is in equilibrium with the excited singlet states of the reaction center. As we have discussed previously (*28*, *35*), energy equilibration between these singlet states occurs primarily on the subpicosecond time scales, with slower energy-transfer processes only playing a minor role in the reaction center dynamics. This equilibrium constant can be modified by changing the pigment−protein interactions in the vicinity of the primary electron donor (via the D1-His198 residue) as well as the ligand to the electron acceptor (via the D1-Gln130 residue). Our findings are summarized in Figure 7.

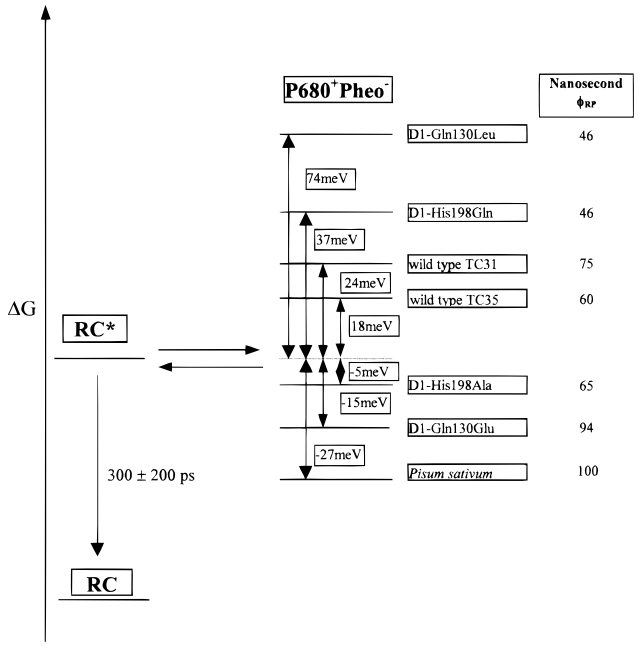

FIGURE 7: Variation of radical pair properties with cation and anion ligands. ϕ_{RP} is determined from the amplitude of the long-lived component on a nanosecond time scale. ΔG is determined at 60 ps from the simulation of the picosecond data in the Q_x region. The estimation of the intrinsic rate of P680* decay is described in the discussion.

The primary radical pair state is formed with a quantum yield of approximately unity in the higher plant reaction center (*25*). If one compares the difference between the total singlet state loss from time-resolved fluorescence data (Table 1, column 6) with the equilibrium population of radical pair states from the Q_x region (column 2) there is a discrepancy (column 7). In particles where the equilibrium population of the radical pair state is low, excited singlet states can be lost without the creation of concomitant radical pairs, for example, the D1-Gln130Leu mutant. In particles where the yield of radical pair formation is higher, the singlet state loss and the extent of radical pair formation are comparable. These findings suggest the presence of a nonradiative decay pathway leading to the loss of the singlet states to ground, which competes with primary charge separation. In the reaction center from *P. sativum*, which has efficient charge separation, this route plays little or no role.

It is possible to simulate the kinetic spectra (sometimes called decay-associated spectra) associated with time constants in the range 18−30 ps by assuming that they are a linear combination of kinetic spectra associated with radical pair formation and kinetic spectra associated with internal conversion of singlet states (see appendix). The results of these simulations reinforce the suggestion that there is a deactivation pathway in action in the PS II reaction center (Table 1, column 8). Although the precision of this analysis is not very high, as it is based on parameters obtained from the fit to the nondecaying components, the general trend is clear.

The nanosecond quantum yield of primary charge separation in the isolated PS II reaction center appears to be related to the average free energy of the radical pair state at 60−80 ps. As the equilibrium constant between the radical pair state and the singlet excited state is shifted toward the excited state, the quantum yield of the primary radical pair formation is decreased (Figure 7). A similar effect has been found in the reaction centers of purple bacteria and PSI. The work of Allen et al. has probed the effect of adding either one, two (*36*, *37*), or three hydrogen bonds to the special pair in *Rb. sphaeroides* (*38*). On adding hydrogen bonds to P870, the free energy of the radical pair state is raised. When three new hydrogen bonds have been formed, the energy of the radical pair state is almost isoenergetic with the singlet excited state. When the free energy of this radical pair state is raised, it is accompanied by a decrease in the quantum yield of primary radical pair formation. This was attributed to a deactivation pathway from the excited state with a rate constant of $(75-300\ \text{ps})^{-1}$. Similarly, in photosystem I, when the histidine-656 ligand to P700 is replaced by serine, an excited-state deactivation pathway has been proposed to occur (*39*). The intrinsic decay time due to internal conversion of excited singlet states (P*) in the LH(L131) mutant which introduces a hydrogen bond between histidine and one of the ring-V, 9-keto groups of primary donor in the *Rb. Sphaeroides* reaction center was estimated to be $(75\ \text{ps})^{-1}$. In the double mutant LH(L131) + LH(M160), which introduces hydrogen bonds to both of the ring-V, 9-keto groups of the primary donor, the intrinsic P* decay rate of $(300\text{ps})^{-1}$ was estimated (*37*). In a mutant where the active pheophytin was absent, the excited-state decayed to ground with a 190 ps time constant (*40*).

If rapid internal conversion of P680* occurs in PSII, then how rapid is this process? Moreover, are all of our observations explained by the shift in the equilibrium constant upon mutation and a fixed rate of RC* deactivation (due to subpicosecond equilibration between P680* and the other reaction center excited singlet states; these states are not distinguishable in the experiments reported here)? From a kinetic model based upon the scheme in Figure 7, it is possible to quantify the equilibrium constant dependence of nonradiative singlet states loss for various intrinsic rates of RC* deactivation. The results of this kinetic modeling suggest that the intrinsic lifetime of RC* *is* changed by mutation of the D1-His198 and D1-Gln130 sites. We can give a crude estimate of the range of internal conversion rates of RC* to be 300 ± 200 ps depending on the identity of the amino acids. One implication of the kinetic modeling is that the quantum yield is slightly less than unity for the reaction center from *P. sativum*. For an intrinsic rate of RC* internal conversion of 300 ps, the quantum yield of charge separation is 0.95. This value is within the error limits of the estimates available from the literature (*25*).

Although rapid internal conversion has been discussed previously in detail for the special pair of the bacterial reaction center, it has not previously been considered in detail for PS II. It is indeed possible that this deactivation pathway may play a role in the regulation of photosystem II function. Given the small free changes associated with charge separation in PS II (*31*, *33*), small perturbations to these energetics may have a large effect. This is clearly exemplified in the results presented here, in which we demonstrate that small changes in the radical pair free energy result in a significant change in the radical pair yield due to changes in the yield of the internal conversion pathway from the RC* states. Our data therefore indicate a viable mechanism of regulation function, which has not previously been addressed.

The most striking finding of this study, which has been confirmed by three independent experimental techniques, is that in *Synechocystis* the quantum yield of primary charge separation can be enhanced above that of the wild-type *Synechocystis* reaction center. This can be achieved by modifications either at the site of the pheophytin anion or in the vicinity of the site of the chlorophyll cation. It is worth noting that the cyanobacterium *Synechococcus* PCC 7942 has two forms of PS II that differ by 25 amino acids in the D1 polypeptide. It has been postulated that this acts as part of its regulatory mechanism. One form is expressed under low light and one under high-light. It has been suggested that the high light form is less easily photoinhibited than the low-light form, thus making a possible regulatory mechanism. Moreover, it was demonstrated that the high-light form of PS II exhibits a 25% higher yield than the low-light form (ref *41*, and references therein). This is particularly interesting because one of the amino acids that changes between the two forms of *Synechococcus* PS II reaction center is the D1−130 residue; in low light it is a glutamine, while in high light it is a glutamate.

CONCLUSIONS

(1) Three time-resolved techniques have been employed regarding the effect of site-directed mutagenesis on the primary photochemistry of PS II. The four independent sets of results from these measurements are quantitatively consistent with each other.

(2) The nanosecond quantum yield of charge separation can be increased or decreased by changing the free energy of the primary radical pair state. This can be done by engineering either the cation or anion binding sites.

(3) Increasing the hydrogen bond strength to the anion lowers the radical pair free energy, and weakening the hydrogen bonds increases the radical pair free energy, as one would expect.

(4) These results further emphasize the dominating effect of the radical pair ↔ Chl* equilibrium and the minor role (if any) of slow energy transfer in these complexes.

(5) There is a fast deactivation pathway in competition with the primary charge separation. There is an inverse correlation between the radical pair free energy and the radical pair quantum yield.

ACKNOWLEDGMENT

We would like to thank Karim Maghlaoui and David Frith for preparing the reaction center samples and Chris Barnett for excellent technical assistance.

REFERENCES

1. Diner, B. A., & Babcock, G. T. (1996) in *Oxygenic Photosynthesis: The Light Reactions* (Ort, D. R., & Yocum, C. F., Eds.) pp 213−247, Kluwer Academic Publishers, Boston, MA.
2. Nanba, O., & Satoh, K. (1987) *Proc. Natl. Acad. Sci. U.S.A. 84*, 109−112.
3. Barber, J., Chapman, D. J., & Telfer, A. (1987) *FEBS Lett. 220*, 67−73.
4. Zheleva, D., Hankamer, B., & Barber, J. (1996) *Biochemistry 35*, 15074−15079.
5. Eijckelhoff, C., & Dekker, J. P. (1995) *Biochim. Biophys. Acta 1231*, 21−28.
6. Hastings, G., Durrant, J. R., Barber, J., Porter, G., & Klug, D. R. (1992) *Biochemistry 31*, 7638−7647.
7. Klug, D. R., Rech, T., Joseph, D. M., Barber, J., Durrant, J. R., & Porter, G. (1995) *Chem. Phys. 194*, 433−442.
8. Booth, P. J., Crystall, B., Ahmad, I., Barber, J., Porter, G., & Klug, D. R. (1991) *Biochemistry 30*, 7573−7586.
9. Crystall, B., Booth, P. J., Klug, D. R., Barber, J., & Porter, G. (1989) *FEBS Lett. 249*, 75−78.
10. Carpenter, S. D., & Vermaas, W. F. J. (1987) *Physiol. Plant. 77*, 446−451.
11. Pakrisi, H., & Vermaas, W. F. J. (1992) in *The Photosystems: Structure, Function and Molecular Biology* (Barber, J., Ed.) pp 231−257, Elsevier Science Publishers, New York.
12. Nixon, P. J., Chisholm, D. A., & Diner, B. A. (1992) in *Plant Protein Engineering* (Shewry, R. R., & Gutteridge, S., Eds.) pp 93−142, Cambridge University Press, Cambridge, U.K.
13. Nixon, P., & Jansson, C. (1996) in *Molecular Genetics of Photosynthesis* (Andersson, B., Salter, A. H., & Barber, J., Eds.) pp 197−224, University Press, Oxford, U.K.
14. Giorgi, L. B., Nixon, P. J., Merry, S. A. P., Joseph, D. M., Durrant, J. R., de-las-Rivas, J., Barber, J., Porter, G., & Klug, D. R. (1996) *J. Biol. Chem. 271*, 2093−2101.
15. Deisenhofer, J., Epp, O., Miki, K., Huber, R., & Michel, H. (1985) *Nature 318*, 618−624.
16. Allen, J. P., Feher, G., Yeates, T. O., Komiya, H., & Rees, D. C. (1987) *Proc. Natl. Acad. Sci. U.S.A. 84*, 5730−5734.
17. Krauss, N., Schubert, W.-D., Klukas, O., Fromme, P., & Witt, H. T. (1996) *Nat. Struct. Biol. 3*, 965−973.
18. Barber, J. (1987) *Trends Biochem. Sci. 12*, 321−326.
19. Rutherford, A. W. (1986) *Biochem. Soc. Trans. 14*, 15−17.
20. Nixon, P. J. (1994) *Proceedings of the BBSRC 2nd Robert Hill Symposium*, pp 8, London, U.K.
21. Bylina, E. J., Kiramaier, C., McDowell, L., Holten, D., & Youvan, D. C. (1988) *Nature 336*, 182−184.
22. Goldsmith, J. O., King, B., & Boxer, S. G. (1996) *Biochemistry 35*, 2421−2428.
23. Nixon, P. J., Trost, J. T., & Diner, B. A. (1992) *Biochemistry 31*, 10859−10871.
24. Coleman, W. J., Nixon, P. J., Vermaas, W. F. J., & Diner, B. A. (1995) in *In Photosynthesis: from Light to Biosphere* (Mathis, P., Ed.) pp 779−782, Kluwer Academic Publishers, Boston, MA.
25. Booth, P. J., Crystall, B., Giorgi, L. B., Barber, J., Klug, D. R., & Porter, G. (1990) *Biochim. Biophys. Acta 1016*, 141−152.
26. Rech, T., Durrant, J. R., Joseph, D. M., Barber, J., Porter, G., & Klug, D. R. (1994) *Biochemistry 33*, 14678−14774.
27. Merry, S. A. P., Kumazaki, S., Tachibana, Y., Joseph, D. M., Porter, G., Yoshihara, K., Durrant, J. R., & Klug, D. R. (1996) *J. Phys. Chem. 100*, 10469−10478.
28. Durrant, J. R., Hastings, G., Joseph, D. M., Barber, J., Porter, G., & Klug, D. R. (1992) *Proc. Natl. Acad. Sci. U.S.A. 89*, 11632−11636.
29. Kumazaki, S., Joseph, D. M., Crystall, B., Tachibana, Y., Durrant, J., Barber, J., Porter, G., Yoshihara, K., & Klug, D. R. (1995) in *Photosynthesis: From light to Biosphere* (Mathis, P., Ed.) pp 883−886, Kluwer Academic Publishers, Boston, MA.
30. Durrant, J. R., Gary Hastings, D., Joseph, M., Barber, J., Porter, G., & Klug, D. R. (1993) *Biochemistry 32*, 8259−8267.
31. Durrant, J. R., Klug, D. R., Kwa, S. L. S., vanGrondelle, R., & Porter, G. (1995) *Proc. Natl. Acad. Sci. U.S.A. 92*, 2472−2477.
32. Oren-Shamir, M., Sai, P. S. M., Edelman, M., & Schertz, A. (1995) *Biochemistry 34*, 5523−5526.
33. Klug, D. R. (1998) *Philos. Trans. R. Soc. London, Ser. A 356*, 1−15.
34. Holzwarth, A. R., Konermann, L., & Gatzen, G. (1997) *J. Phys. Chem. 101*, 2933−2944.
35. Leegwater, J. A., Durrant, J. R., & Klug, D. R. (1997) *J. Phys. Chem. 101*, 7205−7210.

36. Woodbury, N. W., Peloquin, J. M., Alden, R. G., Lin, X., Lin, S., Taguchi, A. K. W., Williams, J. C., & Allen, J. P. (1994) *Biochemistry 33,* 8101−8112.
37. Peloquin, J. M., Williams, J. C., Lin, X., Alden, R. G., Taguchi, A. K. W., Allen, J. P., & Woodbury, N. (1994) *Biochemistry 33,* 8089−8100.
38. Woodbury, N. W., Lin, S., Lin, X., Peloquin, J. M., Taguchi, A. K. W., Williams, J. C., & Allen, J. P. (1995) *Chem. Phys. 197,* 405−421.
39. Melkozernov, A. N., Su, H., Lin, S., Bingham, S., Webber, A. N., & Blankenship, R. E. (1997) *Biochemistry 36,* 2898−2907.
40. Vos, M. H., Lambry, J.-C., Robles, S. J., Youvan, D. C., Breton, J., & Martin, J.-L. (1991) *Proc. Natl. Acad. Sci. U.S.A. 88,* 8885−8889.
41. Oquist, G., Campbell, D., Clarke, A. K., & Gustafsson, P. (1995) *Photosynth. Res. 46,* 151−158.

BI980502D